Ribosomal S6 Kinase 2 Is a Key Regulator in Tumor Promoter–Induced Cell Transformation

Yong-Yeon Cho, Ke Yao, Hong-Gyum Kim, Bong Seok Kang, Duo Zheng, Ann M. Bode, and Zigang Dong

Hormel Institute, University of Minnesota, Austin, Minnesota

Abstract

The ribosomal S6 kinase 2 (RSK2), a member of the $p90^{RSK}$ (RSK) family of proteins, is a widely expressed serine/threonine kinase that is activated by extracellular signal-regulated kinase 1/2 and phosphoinositide-dependent kinase 1 in response to many growth factors and peptide hormones. Its activation signaling enhances cell survival. However, the roles of RSK2 in cell transformation have not yet been elucidated. Here, we found that RSK2 is a critical serine/threonine kinase for the regulation of cell transformation. When cells were stimulated with tumor promoters, such as epidermal growth factor (EGF) or 12-*O*-tetradecanoylphorbol-13-acetate (TPA), phosphorylation of RSK was increased within 5 min. Cell proliferation was suppressed in $RSK2^{-/-}$ mouse embryonic fibroblasts (MEFs) compared with $RSK2^{+/+}$ MEFs. Moreover, $RSK2^{-/-}$ MEFs accumulated at the G_1 phase of the cell cycle under normal cell culture conditions as well as after stimulation with EGF or TPA. In the anchorage-independent cell transformation assay (soft agar), stable expression of RSK2 in JB6 cells significantly enhanced colony formation in either the presence or absence of tumor promoters. Furthermore, knockdown of RSK2 with small interfering RNA-RSK2 suppressed constitutively active Ras (Ras^{G12V})-induced foci formation in NIH3T3 cells. In addition, kaempferol, an inhibitor of RSK2, suppressed EGF-induced colony formation of JB6 Cl41 cells in soft agar, which was associated with inhibition of histone H3 phosphorylation (Ser^{10}). These results showed that RSK2 is a key regulator for cell transformation induced by tumor promoters such as EGF and TPA. [Cancer Res 2007;67(17):8104–12]

Introduction

The mitogen-activated protein kinases (MAPK) are important regulators of proliferation and oncogenesis (1, 2). The MAPK extracellular signal-regulated kinase (ERK) 1/2 (3, 4) mediates the 90-kDa ribosomal S6 kinases (RSK), which are a family of widely expressed serine/threonine kinases that respond to many growth factors, peptide hormones, and neurotransmitters (5, 6). When activated, RSK2 is translocated to the nucleus, where it can phosphorylate various nuclear proteins, including c-Fos, Elk-1, histones, cyclic AMP–responsive element binding protein (CREB; refs. 7–11), activating transcription factor 4 (ATF4; ref. 12), and p53 (13).

The epidermal growth factor (EGF) and phorbol ester, 12-*O*-tetradecanoylphorbol-13-acetate (TPA), are well-known tumor promotion agents used to study malignant transformation in cell and animal models of cancer (14). Either of these two agents can induce activation of the transcription factor activator protein-1 (AP-1; refs. 15, 16). When treated with TPA or EGF, JB6 Cl41 skin epidermal cells show an induction of AP-1 transcriptional activation in promotion-sensitive (P^+) phenotypes but not in promotion-resistant (P^-) phenotypes (17). Blocking AP-1 activation causes P^+ cells to revert to the P^- phenotype, indicating a unique requirement for AP-1 activation in TPA- or EGF-induced cell transformation (18).

Recent studies have indicated that RSK2 is involved in the survival of neurons that have been treated with a survival growth factor, brain-derived neutrophic factor, mediated through phosphorylation of the proapoptotic protein BAD (Ser^{112}; ref. 19). Moreover, RSK2 knockout mice display reduction of c-Fos–dependent osteosarcoma formation through the regulation of c-Fos protein stability (20). Furthermore, SL0101, a selective RSK2 inhibitor extracted from the tropical plant *Forsteronia refracta*, has been shown to inhibit RSK2 activity and suppress proliferation of MCF-7 breast cancer cells or LNCaP prostate cancer cells (21, 22). Although RSK2 is believed to be involved in cancer cell proliferation and osteosarcoma development (20–22), a role for RSK2 in cell transformation induced by tumor promoters, such as EGF or TPA, has not been reported.

Here, we showed that RSK2 is a key regulator for tumor promoter–induced cell transformation. Ectopic expression of RSK2 in JB6 Cl41 cells caused increased proliferation as well as anchorage-independent transformation. Furthermore, knockdown of RSK2 by siRNA almost totally blocked foci formation in NIH3T3 cells. These results showed that RSK2 is a key regulator of cell transformation induced by tumor promoters such as EGF or TPA.

Materials and Methods

Reagents and antibodies. Chemical reagents, including Tris, NaCl, and SDS, for molecular biology and buffer preparation were purchased from Sigma-Aldrich. Restriction enzymes and some modifying enzymes were purchased from New England Biolabs, Inc. The Taq DNA polymerase was obtained from Qiagen, Inc. The DNA ligation kit (version 2.0) was purchased from TAKATA Bio, Inc. and the pcDNA4-HisMaxA plasmid used for the construction of the expression vector was from Invitrogen. Cell culture medium and other supplements were purchased from Life Technologies, Inc. Antibodies for Western blot analysis were purchased from Cell Signaling Technology, Inc., Santa Cruz Biotechnology, Inc., or Upstate Biotechnology, Inc.

Construction of pHisG-RSK2 and psi-RSK2. The RSK2 coding fragment, including the open reading frame, was constructed previously (13), and the *Bam*HI/*Xba*I fragment from pBIND-RSK2 was introduced into the *Bam*HI/*Xba*I site of pcDNA4-HisMaxA (pHisG-RSK2). To construct the small interfering RNA (siRNA)-RSK2 (psi-RSK2), the pU6pro vector (a gift kindly provided by Dr. David L. Turner, Mental Health Research Institute,

Note: Supplementary data for this article are available at Cancer Research Online (http://cancerres.aacrjournals.org/).

Requests for reprints: Zigang Dong, Hormel Institute, University of Minnesota, 801 16th Avenue Northeast, Austin, MN 55912. Phone: 507-437-9600; Fax: 507-437-9606; E-mail: zgdong@hi.umn.edu.

doi:10.1158/0008-5472.CAN-06-4668

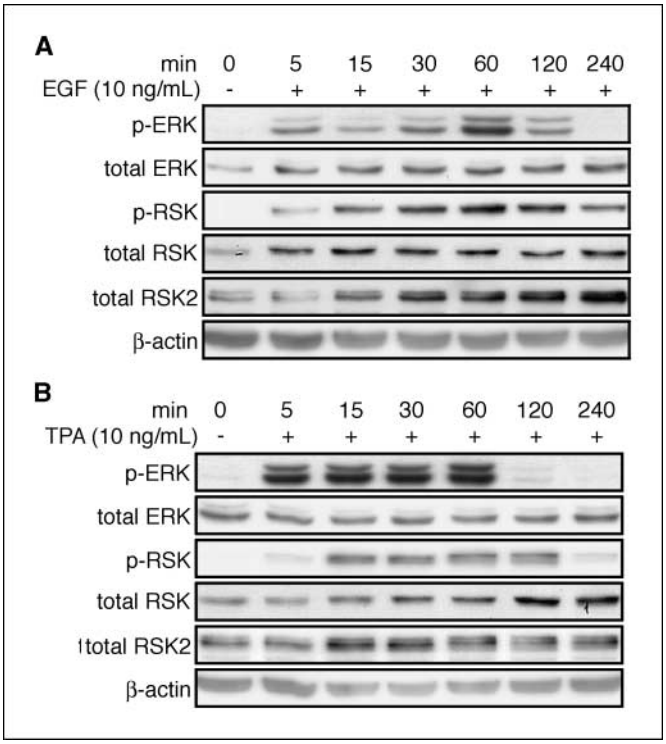

Figure 1. RSK2 is regulated by tumor promoters such as EGF and TPA. HaCat cells (1×10^6) were seeded into 10-cm dishes and then cultured overnight. Cells were subsequently starved in 0.1% FBS-DMEM for 24 h and then stimulated with 10 ng/mL EGF (*A*) or 10 ng/mL TPA (*B*) and harvested at the indicated time point. The proteins were extracted with NP40 cell lysis buffer and Western blotting was conducted as described in Materials and Methods using specific antibodies as indicated. Equal protein loading was confirmed using the β-actin antibody on the same membrane. *p-ERK,* phosphorylated ERK; *p-RSK,* phosphorylated RSK.

University of Michigan, Ann Arbor, MI) was digested with *Xba*I and *Bbs*I. The annealed synthetic primers were then introduced following the recommended protocols.[1] The recombinant plasmids of pHisG-RSK2 and psi-RSK2 were confirmed by agarose gel electrophoresis and DNA sequencing.

Cell culture and transfections. HaCat, $RSK2^{+/+}$, and $RSK2^{-/-}$ mouse embryonic fibroblasts (MEFs; a generous gift from Dr. J.C. Bruning, Institute for Genetics, Center for Molecular Medicine Cologne, Cologne, Germany) were cultured with DMEM supplemented with 10% fetal bovine serum (FBS) and antibiotics at 37°C in a 5% CO_2 incubator. JB6 Cl41 mouse skin epidermal cells were cultured in 5% FBS-MEM. NIH3T3 cells were cultured 10% calf serum in DMEM. The cells were maintained by splitting at 90% confluence and media were changed every 3 days. When cells reached 50% to 60% confluence, transfection of the expression vectors was done using LipofectAMINE (Life Technologies) following the manufacturer's suggested protocol.

3-(4,5-Dimethylthiazol-2-yl)-5-(3-carboxymethoxyphenyl)-2-(4-sulfophenyl)-2H-tetrazolium assay. To estimate cell proliferation, $RSK2^{+/+}$ and $RSK2^{-/-}$ MEFs were seeded (1×10^3) into 96-well plates in 100 μL of 10% FBS-MEM and incubated in a 37°C, 5% CO_2 incubator. JB6 Cl41 cells stably transfected with the mock vector or pHisG-RSK2 were seeded (1×10^3) into 96-well plates in 100 μL of 5% FBS-MEM and incubated in a 37°C, 5% CO_2 incubator. After culturing for 12 h, 20 μL of the CellTiter96 Aqueous One Solution (Promega) were added to each well and cells were then incubated for 1 h at 37°C and 5% CO_2. To stop the reaction, 25 μL of a 10% SDS solution were added and absorbance was measured at 490 and 690 nm.

Anchorage-independent cell transformation assay. EGF- or TPA-induced cell transformation was investigated in mock or pHisG-RSK2 stably transfected cells. In brief, cells (8×10^3/mL) were exposed to EGF (0.1–10 ng/mL) or TPA (0.1–10 ng/mL) in 1 mL of 0.3% basal medium Eagle (BME) agar containing 10% FBS. The cultures were maintained in a 37°C, 5% CO_2 incubator for 10 days (EGF) or 3 to 4 weeks (TPA), and the cell colonies were scored using a microscope and the Image-Pro PLUS (version 4) computer software program (Media Cybernetics) as described by Colburn et al. (23).

Focus-forming assay. Transformation of NIH3T3 cells was conducted according to standard protocols (24). Cells were transiently transfected with combinations of pcDNA3-H-Ras^{G12V} (50 ng), pHisG-RSK2 (450 ng), psi-RSK2 (450 ng) DNA, and pcDNA3-mock (compensation to achieve equal amount of DNA) DNA and then cultured in 5% FBS-DMEM for 2 weeks. Foci were fixed and stained with 0.5% crystal violet and counted with a microscope and the Image-Pro PLUS (version 4) software program.

Cell cycle analysis. $RSK2^{+/+}$ or $RSK2^{-/-}$ MEFs (2×10^5) were seeded into 60-mm dishes and cultured for 36 h at 37°C in a 5% CO_2 incubator. The cell was starved for 24 h with 0.1% FBS-DMEM and then stimulated with EGF (10 ng/mL) or TPA (10 ng/mL) for 12 h. The cells were harvested with trypsin, fixed with ethanol, stained with propidium iodide, and then analyzed for cell cycle phase by flow cytometry.

***In vitro* kination assay.** GST-NFAT3D4-261-365 or GST-CREB2 protein was used for an *in vitro* kination assay with active RSK2 (Upstate Biotechnology). Reactions were carried out at 30°C for 30 min in a mixture containing 10 μmol/L unlabeled ATP and 10 μCi [γ-^{32}P]ATP and then stopped by adding 6× SDS sample buffer. For the inhibitory effect of kaempferol on RSK2 activity, we used 10 μmol/L unlabeled ATP and 10 μCi [γ-^{32}P]ATP. Samples were boiled and then separated by 12% SDS-PAGE and visualized by autoradiography, Western blotting, or Coomassie blue staining.

Western blotting. Samples containing equal amounts of protein were resolved by the appropriate percentage SDS-PAGE and transferred onto polyvinylidene difluoride (PVDF) membranes. The membranes were incubated in blocking buffer and then probed with specific primary antibodies against phosphorylated ERK, phosphorylated RSK, total ERK, total histone H3 (Cell Signaling Technology), total RSK2, phosphorylated histone H3 (Upstate Biotechnology), or β-actin (Sigma-Aldrich) and the appropriate anti-rabbit or anti-mouse horseradish peroxidase (HRP) as the secondary antibody. The Western blots were visualized using an enhanced chemiluminescence (ECL) detection system (Amersham Biosciences Corp.).

Extraction of nuclear and cytoplasmic fractions. To analyze histone H3 phosphorylation, $RSK2^{+/+}$, $RSK2^{-/-}$, and JB6 Cl41 cells were seeded in 10-cm dishes and cultured to about 90% to 95% confluence. The cells were starved for 24 h and then stimulated with EGF (10 ng/mL) either with or without various concentrations of kaempferol over different times. The cells were harvested and nuclear and cytoplasmic fractions were extracted with the NE-PER nuclear and cytoplasmic extraction reagents (Pierce) following the manufacturer's suggested protocols. To obtain nuclear extracts containing histone H3, the nuclear fractions were treated with 250 units benzonase (Sigma-Aldrich) for 30 min on ice. Samples were mixed for 15 s by vortex every 10 min and the supernatant fraction was recovered by centrifugation (13,000 rpm, 5 min at 4°C). The supernatant fraction was the nuclear fraction containing histone proteins. To detect histone H3 phosphorylation (Ser^{10}) and total histone H3 protein, 2 μg of total nuclear fraction protein were used for Western blot analysis.

Results

RSK is regulated by the tumor promoters EGF or TPA. The MAPK signaling pathway not only promotes cell proliferation but also mediates cell survival and is up-regulated in various cancer cells (25). We hypothesized that RSK, which is an ERK downstream serine/threonine protein kinase, might play a key role in cell transformation. To examine whether RSK is regulated by tumor promoters, such as EGF or TPA, HaCat cells were starved for

[1] http://sitemaker.umich.edu/dlturner.vectors

24 h with 0.1% FBS-DMEM and then stimulated with EGF (10 ng/mL) or TPA (10 ng/mL). Results indicated that phosphorylation and activation of ERK were increased at 5 min, maintained to 60 min, and decreased at 120 min after EGF or TPA treatment (Fig. 1*A* and *B*). The phosphorylation of RSK was first detected at 5 min, gradually increased to 120 min, and then decreased at 240 min after EGF or TPA treatment (Fig. 1*A* and *B*). Total RSK protein level was also increased in a time-dependent manner with EGF or TPA treatment (Fig. 1*A* and *B*). Furthermore, the RSK2 protein level was increased in a manner similar to ERK and RSK. These results indicated that the tumor promoters EGF and TPA activated the ERK-RSK signaling pathway, including RSK2.

RSK2 deficiency suppresses cell proliferation by causing accumulation of cells at G_1. The Ras-ERK signaling pathway regulates cell survival (25) and the MAPK cascades are implicated in the regulation of cell proliferation, survival, growth and motility (26, 27), as well as tumorigenesis (28). We hypothesized that RSK2 deficiency would affect cell proliferation. To examine this idea, we confirmed the RSK2 protein level in $RSK2^{+/+}$ and $RSK2^{-/-}$ MEFs by Western blot (Fig. 2*A*). The RSK2 protein was confirmed to be absent in $RSK2^{-/-}$ MEFs. Therefore, we analyzed proliferation in cells cultured under normal conditions with 10% FBS. The results indicated that RSK2 deficiency suppressed cell proliferation by ~41% compared with $RSK2^{+/+}$ MEFs (Fig. 2*B*). Moreover, we found

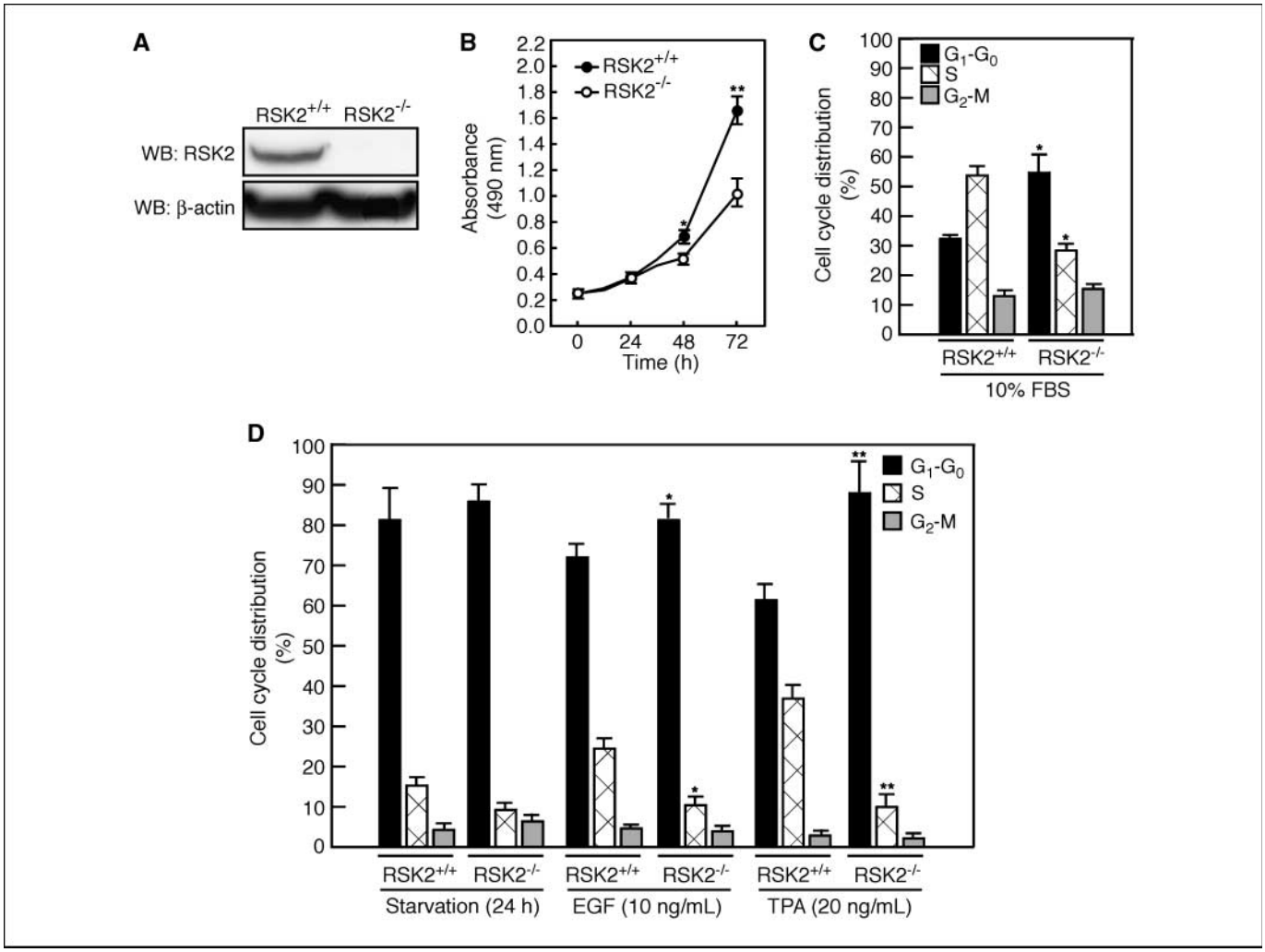

Figure 2. RSK2 deficiency suppresses cell proliferation by causing accumulation of cells in the G_1 phase. *A,* Western blot (*WB*) showing RSK2 expression in $RSK2^{+/+}$ and $RSK2^{-/-}$ MEFs. Cells were cultured in 10% FBS-DMEM and then proteins were extracted by freezing and thawing in NP40 cell lysis buffer. Proteins were resolved by SDS-PAGE and then transferred onto PVDF membranes. Membranes were hybridized with an RSK2 antibody and the appropriate secondary antibody and then visualized using the ECL detection kit. Equal protein loading was confirmed using the β-actin antibody on the same membrane. *B,* $RSK2^{+/+}$ and $RSK2^{-/-}$ MEFs were seeded (1×10^3 per well) into 96-well plates in 100 μL of 10% FBS-DMEM and proliferation was assessed using the CellTiter96 Aqueous One Solution detection kit. Cell proliferation was estimated by absorbance (A_{490}) read at 24-h intervals up to 72 h. *Points,* mean of values obtained from triplicate experiments; *bars,* SD. Statistical differences were evaluated using the Student's *t* test. *Asterisks,* significant difference between $RSK2^{+/+}$ and $RSK2^{-/-}$ MEFs (*, $P < 0.05$ and **, $P < 0.005$). *C,* $RSK2^{+/+}$ and $RSK2^{-/-}$ MEFs (2×10^5 cells) were seeded into 60-mm dishes and cultured for 36 h. The cells were harvested, fixed with ethanol, stained with propidium iodide, and then analyzed for cell cycle phase. Data are expressed as the percentage of cells in G_1-G_0, S, or G_2-M phase. *Columns,* mean of values obtained from triplicate experiments; *bars,* SD. Statistical differences were evaluated using the Student's *t* test. *Asterisk,* significant change in cell cycle phase distribution in $RSK2^{-/-}$ cells compared with $RSK2^{+/+}$ cells (*, $P < 0.01$). *D,* $RSK2^{+/+}$ and $RSK2^{-/-}$ MEFs (2×10^5 cells) were seeded into 60-mm dishes and cultured for 36 h. The cells were starved in 0.1% FBS-DMEM for 24 h and then stimulated with EGF (10 ng/mL) or TPA (10 ng/mL) for an additional 12 h. The cells were harvested, fixed with ethanol, stained with propidium iodide, and then analyzed for cell cycle phase. Data are expressed as the percentage of cells in G_1-G_0, S, or G_2-M phase. *Columns,* mean of values obtained from triplicate experiments; *bars,* SD. Statistical differences were evaluated using the Student's *t* test. *Asterisks,* significant change in cell cycle phase distribution in $RSK2^{-/-}$ cells compared with $RSK2^{+/+}$ cells (*, $P < 0.05$ and **, $P < 0.005$).

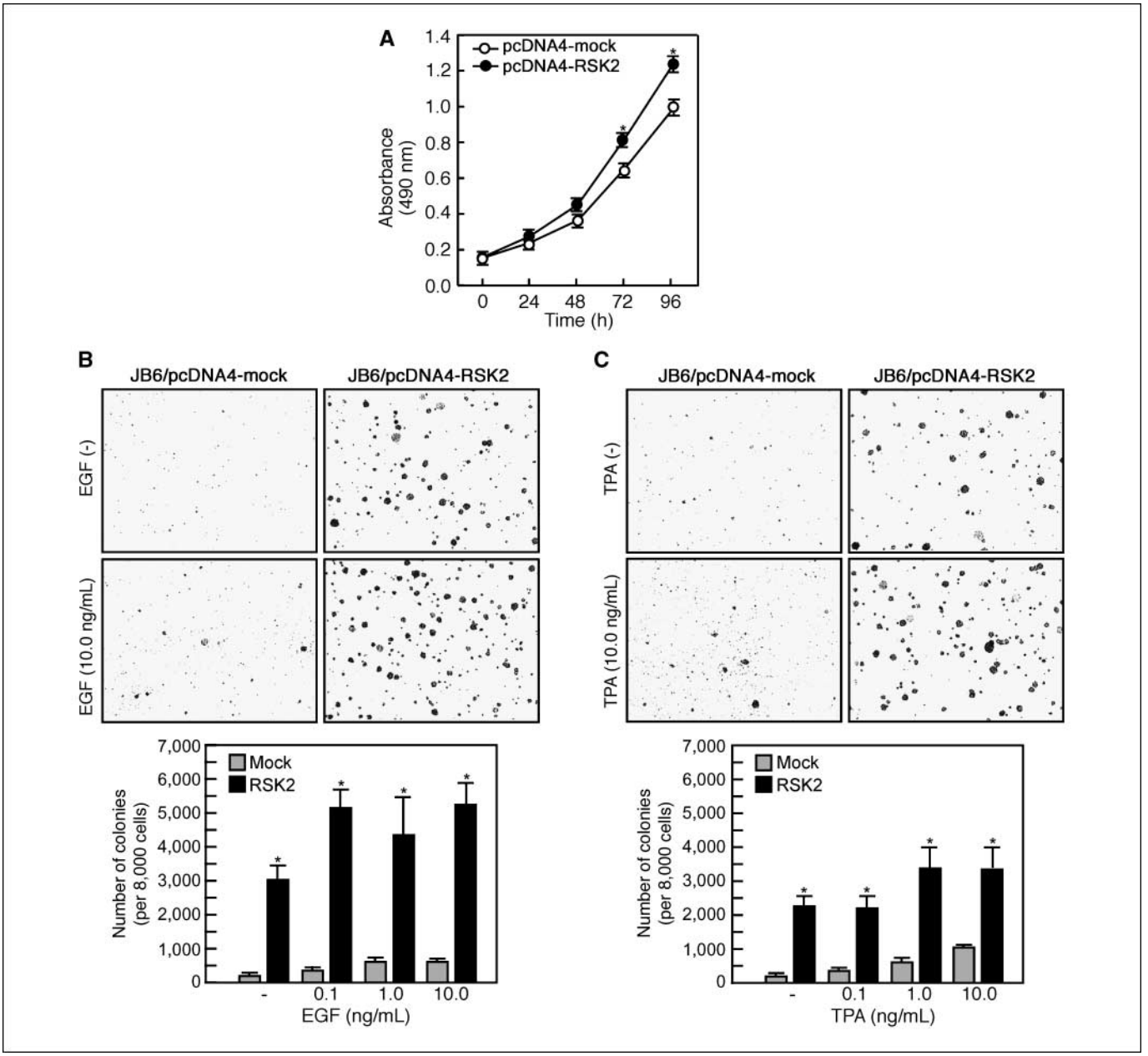

Figure 3. Ectopic expression of RSK2 induces anchorage-independent cell transformation. *A,* ectopic expression of RSK2 increases cell proliferation. Stable transfectants of JB6 Cl41 cells expressing pcDNA4-mock or pHisG-RSK2 were seeded (1×10^3 per well) into 96-well plates in 100 μL of 5% FBS-DMEM and proliferation was assessed using the CellTiter96 Aqueous One Solution detection kit. Cell proliferation was estimated by reading the absorbance (A_{490}) at 24-h intervals up to 96 h. *Points,* mean of values obtained from triplicate experiments; *bars,* SD. Significant differences were evaluated using the Student's *t* test. *Asterisk,* significant difference (*, $P < 0.01$). *B* and *C,* cells (1×10^3/mL) transfected with mock vector or pHisG-RSK2 were exposed to EGF (0–10.0 ng/mL; *B*) or TPA (0–10 ng/mL; *C*) in 1 mL of 0.3% BME agar containing 10% FBS. The cultures were maintained in a 37°C, 5% CO_2 incubator for 10 d and then colonies were counted using a microscope and the Image-Pro PLUS (version 4) computer software program. *B* and *C, bottom, columns,* mean of values obtained from triplicate experiments; *bars,* SD. Significant differences were evaluated using the Student's *t* test. *Asterisk,* significantly higher number of colonies in RSK2-transfected cells compared with mock-transfected cells (*, $P < 0.005$).

that RSK2$^{-/-}$ MEFs showed less cells in S phase and a greater accumulation of cells in the G_1-G_0 phase of the cell cycle compared with RSK2$^{+/+}$ MEFs (Fig. 2*C*). Stimulation with EGF or TPA resulted in a stimulation of cells in S phase for RSK2$^{+/+}$ MEFs but had no effect on the cell cycle progression of RSK2$^{-/-}$ MEFs (Fig. 2*D*). These results clearly showed that RSK2 deficiency suppressed cell proliferation because of an impaired G_1-S cell cycle transition.

Ectopic expression of RSK2 induces anchorage-independent cell transformation. The MAPK pathway controls the growth and survival of a broad spectrum of human tumors. Mutations in Ras or Raf result in activation of the MAPK pathway and are present in a large percentage of solid tumors (25). As indicated above, RSK2 plays an important role in cell proliferation and cell cycle regulation (Fig. 2). Therefore, we hypothesized that RSK2 might play a key role in cell transformation. To examine this idea, we established stably expressed RSK2 in JB6 Cl41 cells and analyzed cell proliferation. The results showed that RSK2 expression increased cell proliferation (Fig. 3*A*), which supported our previous

results (Fig. 2*B*). Mock or RSK2 stable cell lines were subjected to the soft agar assay with stimulation by EGF (10 ng/mL) or TPA (10 ng/mL) to assess cell transformation. Surprisingly, RSK2-overexpressing JB6 Cl41 cells showed about a 15-fold increase in anchorage-independent colony formation even without EGF or TPA stimulation compared with mock JB6 Cl41 stable cells (Fig. 3*B* and *C, top*). Furthermore, EGF or TPA stimulation further increased colony formation in soft agar in a dose-dependent manner (Fig. 3*B* and *C, bottom*). These results showed that RSK2 plays an important role in cell transformation.

Knockdown of RSK2 blocks foci formation. To examine the role of endogenous RSK2 in cell transformation, we designed siRNA against RSK2 (si-RSK2) and a general scrambled mock control (si-mock; Fig. 4*A*) for transfection into NIH3T3 cells. Western blot results revealed that si-RSK2 down-regulated the endogenous RSK2 protein level by ~85% (Fig. 4*B*). To test the effect of knocking down RSK2 on constitutively active Ras (Ras^{G12V})-induced cell transformation, we transfected various combinations of the expression vectors into NIH3T3 cells and then analyzed the effect on foci formation. The results showed that, as expected, Ras^{G12V} induced cell transformation in NIH3T3 cells (Fig. 4*C, top right* and *graph*). Moreover, coexpression of Ras^{G12V} and RSK2 induced even more foci formation in NIH3T3 cells (Fig. 4*C, bottom left* and *graph*). Importantly, cotransfection of si-RSK2 with Ras^{G12V} or Ras^{G12V}/RSK2 almost totally blocked foci formation in NIH3T3 cells (Fig. 4*C, bottom middle* and *right* and *graph*). These results further showed that RSK2 plays a key role in cell transformation. To examine whether the inhibitory effect of RSK2 knockdown on foci formation was related to a suppression of cell proliferation, we established NIH3T3 cells stably expressing Ras^{G12V} or mock. The mock or Ras^{G12V} stable cells were then reintroduced with si-mock (mock/si-mock or Ras/si-mock) or si-RSK2 (mock/si-RSK2 or Ras/si-RSK2), respectively, and cell proliferation was then analyzed. The results indicated that si-RSK2 transfection into the mock stable cell line (mock/si-RSK2) suppressed cell proliferation by ~20% compared with si-mock control cells (mock/si-mock; Fig. 4*D*). Notably, Ras^{G12V} stable cells transfected with si-mock (Ras/si-mock) showed an increase in cell proliferation by ~16% compared with the mock stable cell line (mock/si-mock; Fig. 4*D*). However, introducing si-RSK2 into Ras^{G12V} stable cells (Ras/si-RSK2) suppressed cell proliferation to a level about the same as the mock stable cell line (mock/si-mock; Fig. 4*D*). Taken together, we

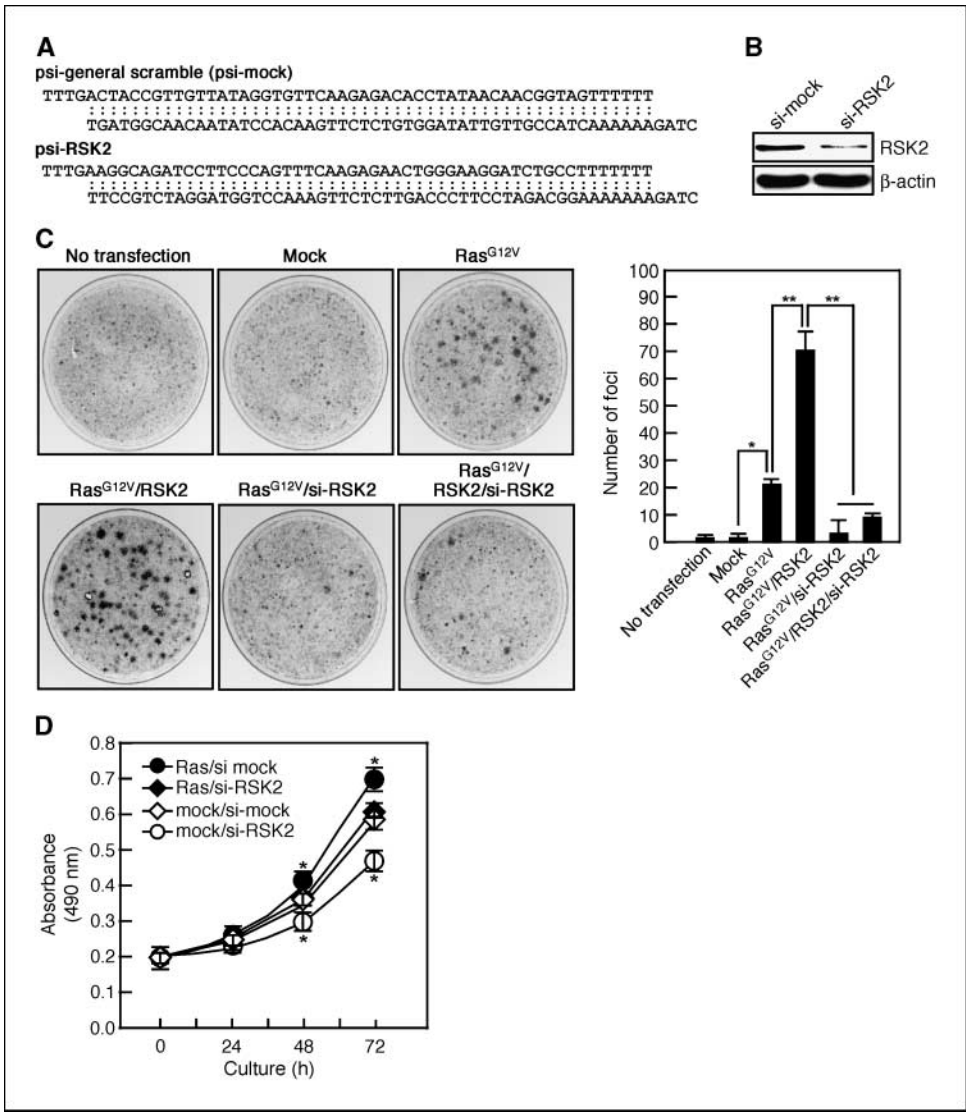

Figure 4. Knockdown of RSK2 blocks focus formation. *A,* nucleotide alignment of si-mock and si-RSK2 primer sequences. *B,* si-RSK2 efficiently suppresses the endogenous RSK2 protein level. NIH3T3 cells (60% confluence) were transfected with psi-general scramble (psi-mock) or psi-RSK2 and cultured for 36 h. Proteins were extracted with NP40 cell lysis buffer and Western blotting was conducted as described in Materials and Methods using specific antibodies as indicated. Equal protein loading was confirmed using the β-actin antibody on the same membrane. *C,* knockdown of RSK2 blocks Ras-induced focus formation. A focus-forming assay was done by following standard protocols as described in Materials and Methods. Foci were stained with 0.5% crystal violet and counted under a microscope using the Image-Pro PLUS (version 4) software program. *Right,* number of foci. *Columns,* mean of values obtained from triplicate experiments; *bars,* SD. Significant differences were evaluated using the Student's *t* test. *Asterisks,* significant difference in foci formation (*, $P < 0.01$ and **, $P < 0.001$). *D,* NIH3T3 cells stably expressing pcDNA3-Ras^{G12V} (Ras) or pcDNA3-mock (mock) were transiently transfected with si-mock or si-RSK2, respectively. The cells were cultured for 24 h in a 5% CO_2 incubator and then seeded into 96-well plates (1×10^3 per well in 100 μL of 10% calf serum-DMEM), and proliferation was assessed using the CellTiter96 Aqueous One Solution detection kit. Cell proliferation was estimated by reading the absorbance (A_{490}) at 24-h intervals up to 72 h. *Points,* mean of values obtained from six replicate experiments; *bars,* SD. Significant differences were evaluated using the Student's *t* test. *Asterisk,* significant difference compared with mock/si-mock cells (*, $P < 0.01$).

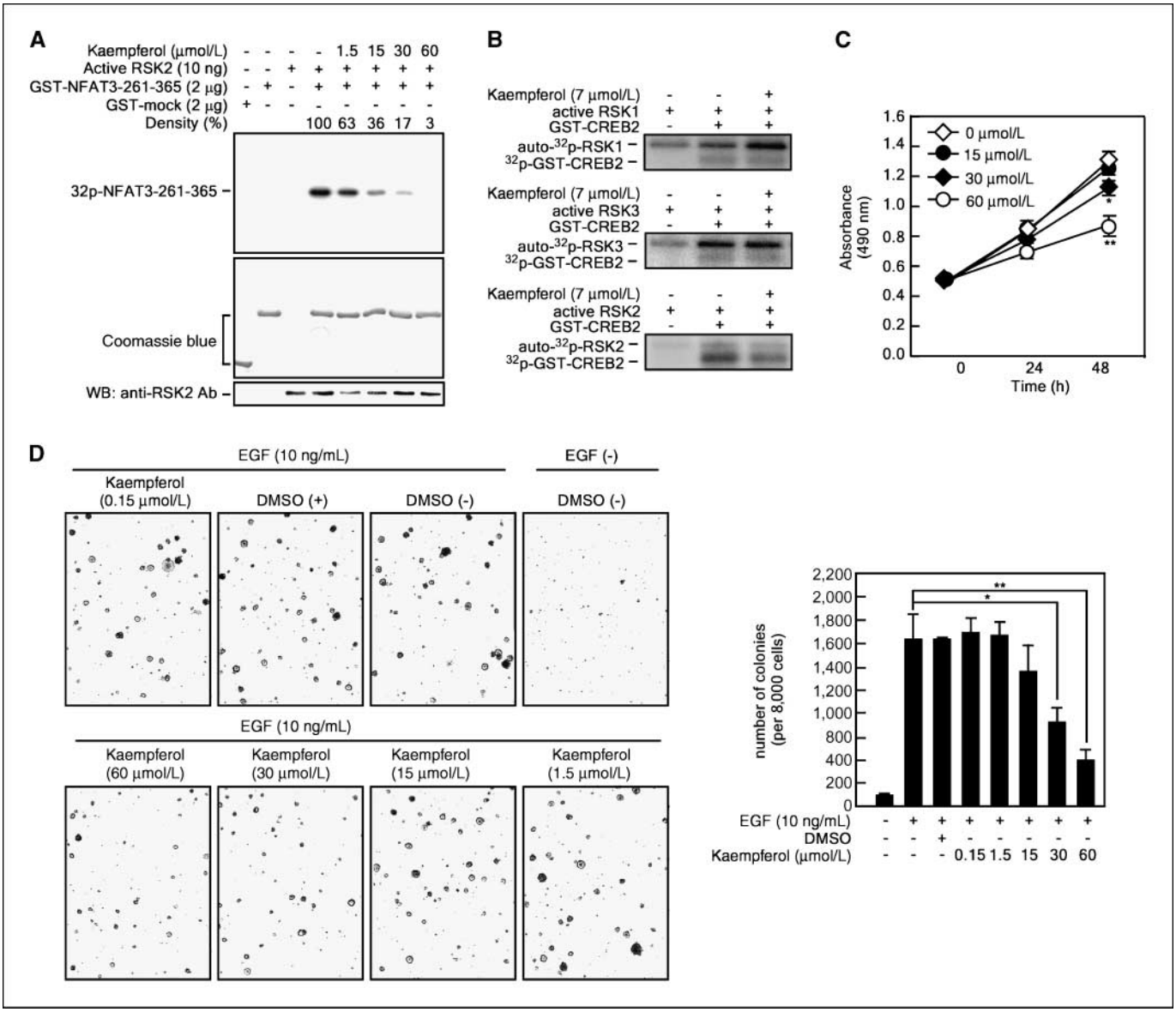

Figure 5. Kaempferol, an inhibitor of RSK2, suppresses proliferation and EGF-induced transformation in JB6 Cl41 cells. *A,* kaempferol inhibits RSK2 activity *in vitro*. Active RSK2 (10 ng) was combined with GST-NFAT3-261-365 (2 μg), 10 μmol/L unlabeled ATP, 10 μCi [γ-^{32}P]ATP, and the indicated dose of kaempferol. An *in vitro* phosphorylation assay was carried out as described in Materials and Methods. Band density was measured using the ImageJ computer program and band intensity of active RSK2 and GST-NFAT3-261-365 (100%) was compared. *B,* specificity of kaempferol. Active RSK1, RSK3, or RSK2 (10 ng of each) was combined with 20 ng GST-CREB2, 10 μmol/L unlabeled ATP, 10 μCi [γ-^{32}P]ATP, and 7 μmol/L kaempferol. The kinase reaction was carried out as described in Materials and Methods. The ^{32}P radioisotope-labeled GST-CREB2 protein bands were visualized by autoradiography. *C,* kaempferol suppresses cell proliferation. JB6 Cl41 cells (8×10^3) were seeded into 96-well plates and cultured for 12 h. The cells were treated with the indicated concentrations of kaempferol (0–60 μmol/L in DMSO) and proliferation was determined using the CellTiter96 Aqueous One Solution detection kit. Cell proliferation was estimated by reading absorbance (A_{490}) at 24-h intervals up to 48 h. The quenching of chemical background for absorbance was obtained by subtracting the absorbance value of kaempferol-treated medium without cells from the kaempferol-treated medium with cells. *Points,* mean of values obtained from six replicate experiments; *bars,* SD. Significant differences were evaluated using the Student's *t* test. *Asterisk,* significant decrease in proliferation by concentration (*, $P < 0.05$ and **, $P < 0.005$). *D,* kaempferol suppresses EGF-induced anchorage-independent colony formation in soft agar. Cells (8×10^3/mL) were exposed to EGF (10.0 ng/mL) with different doses of kaempferol in 1 mL of 0.3% BME agar containing 10% FBS. The cultures were maintained in a 37°C, 5% CO_2 incubator for 10 d and then colonies were counted using a microscope and the Image-Pro PLUS (version 4) computer software program. *Columns,* mean of values obtained from triplicate experiments; *bars,* SD. Significant differences were evaluated using the Student's *t* test. *Asterisks,* significant inhibitory effect of kaempferol on EGF-induced cell transformation (*, $P < 0.01$ and **, $P < 0.005$).

concluded that the inhibitory effect on cell proliferation induced by RSK2 knockdown is at least partially involved in the observed reduction of cell transformation.

Kaempferol, an inhibitor of RSK2, suppresses cell proliferation and EGF-induced transformation of JB6 Cl41 cells. Flavonoids, including myricetin, quercetin, kaempferol, luteolin, and apigenin, are well-known compounds found in editable tropical plants. The highest total flavonoid content is found in onion leaves (quercetin at 1,497.5 mg/kg; luteolin at 391.9 mg/kg, and kaempferol at 832.0 mg/kg; ref. 29). Kaempferol has been shown to inhibit RSK2 activity (21, 30) and was used in the present studies to assess the role of RSK2 in cell proliferation and anchorage-independent cell transformation. We first determined whether kaempferol can inhibit RSK2 activity by testing the effect

on RSK2 kinase activity *in vitro* toward the NFAT3 protein, which is a novel substrate of RSK2 (Supplementary Fig. S1; ref. 31). We found that kaempferol inhibited RSK2 in a dose-dependent manner (Fig. 5*A*). Next to examine whether kaempferol has specificity for RSKs, we constructed a GST-CREB2 fusion expression vector (pGST-CREB2), which is a common substrate of RSKs (Supplementary Fig. S2). This was expressed in *BL21* and partially purified and then directly subjected to an *in vitro* kinase assay with RSK1, RSK2, or RSK3 using [γ-^{32}P]ATP and 7 μmol/L kaempferol. This concentration of kaempferol was shown to be effective in inhibiting RSK2 activity by ~50% (Fig. 5*A* and *B, bottom*) but had no effect on RSK1 or RSK3 activity (Fig. 5*B, top* and *middle*). These results indicated that kaempferol has a specific inhibitory effect on RSK2 at this concentration. The toxicity of kaempferol against JB6 Cl41 cells (8×10^4 per well in 96-well plates) was assessed over varying periods. Results indicated that the highest concentration of kaempferol (60 μmol/L) had no cytotoxic effect at 48 h after treatment (Supplementary Fig. S3). Next to examine whether kaempferol can inhibit cell proliferation, we analyzed cell proliferation with different doses of kaempferol over varying periods. The results showed that kaempferol suppressed cell growth in a concentration-dependent manner (Fig. 5*C*) and cell death was not observed (data not shown). Therefore, we concluded that doses of kaempferol up to 60 μmol/L were not toxic but inhibited cell proliferation. We next investigated the effect of kaempferol on EGF-stimulated colony formation in the anchorage-independent cell transformation assay. JB6 Cl41 cells were stimulated with EGF (10 ng/mL) with or without a combination of different doses of kaempferol for 10 days. The results showed that EGF and/or DMSO alone had no effect on colony formation (Fig. 5*D*). On the other hand, kaempferol had an inhibitory effect of ~44% at 30 μmol/L and 75% at 60 μmol/L concentrations (Fig. 5*D, right* and *graph*). These results indicated that kaempferol suppressed cell proliferation as well as EGF-induced cell transformation.

RSK2 is a key regulator of histone H3 phosphorylation. Our previous studies indicated that RSK2 phosphorylated histone H3 at Ser^{10} when induced by EGF or UVB (13). Furthermore, the phosphorylation of histone H3 at Ser^{10} was shown to be indispensable for neoplastic cell transformation induced by EGF (32). Therefore, we examined the inhibitory effect of kaempferol on RSK2 by analyzing histone H3 phosphorylation (Ser^{10}) *in vivo*. Results confirmed that EGF induced histone H3 phosphorylation (Ser^{10}; Fig. 6*A*). Moreover, we found that EGF-induced histone H3 phosphorylation (Ser^{10}) was inhibited by ~50% by treatment with

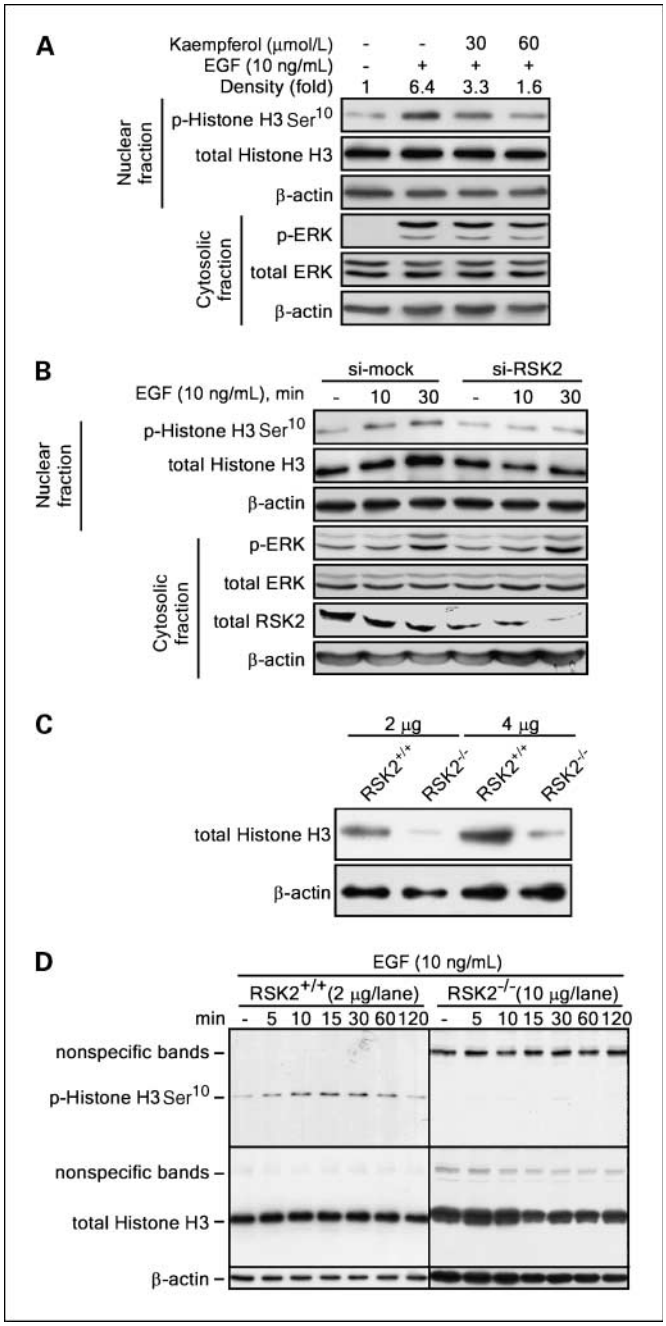

Figure 6. Histone H3 phosphorylation at Ser^{10} is eliminated by inhibition of RSK2. *A,* kaempferol inhibits histone H3 phosphorylation at Ser^{10}. JB6 Cl41 cells (1×10^6) were seeded into 10-cm dishes in 5% FBS-MEM and cultured until cells reached 90% to 95% confluence. The cells were starved for 24 h in 0.1% FBS-MEM and then stimulated with EGF (10 ng/mL) for 15 min and subsequently harvested. The nuclear and cytosolic fractions were extracted with NE-PER nuclear and cytoplasmic extraction reagents (Pierce) following the manufacturer's suggested protocols. To extract histone proteins, the nuclear fraction was treated with benzonase (250 units) for 30 min on ice and then the supernatant fraction was recovered by centrifugation. The nuclear fraction containing histone proteins was used for histone H3 detection and the cytosolic fraction was used for detection of ERK by Western blotting as described in Materials and Methods. Equal protein loading was confirmed using the β-actin antibody on the same membrane. *B,* RSK2 knockdown suppresses EGF-induced histone H3 phosphorylation at Ser^{10}. NIH3T3 cells were transfected with psi-mock or psi-RSK2, cultured and starved each for 24 h, and then stimulated with EGF (10 ng/mL). The cells were harvested at the indicated time point and histone protein was extracted as described for (*A*). Phosphorylated and total histone H3 proteins were visualized from the nuclear fraction by Western blotting using specific antibodies. The phosphorylated ERK, total ERK, and total RSK2 proteins were visualized from the cytosolic fraction by Western blotting with specific antibodies and equal protein loading was confirmed using the β-actin antibody on the same membrane. *C,* RSK2$^{-/-}$ MEFs contain lower levels of the histone H3 protein. Histone proteins were extracted from RSK2$^{+/+}$ and RSK2$^{-/-}$ MEFs as described for (*A*). Total proteins (2 or 4 μg) were resolved by 15% SDS-PAGE, transferred onto PVDF membranes, and visualized using a total histone H3 antibody and HRP-conjugated secondary antibody as described in Materials and Methods. Equal protein loading was confirmed using the β-actin antibody on the same membrane. *D,* RSK2 deficiency blocks EGF-induced histone H3 phosphorylation at Ser^{10}. RSK2$^{+/+}$ and RSK2$^{-/-}$ MEFs (1×10^6) were seeded into 10-cm dishes, cultured to about 90% to 95% confluence, and subsequently starved in 0.1% FBS-DMEM for 24 h. The cells were stimulated with EGF (10 ng/mL) and harvested at the indicated time point, and then histone proteins were extracted as described for (*A*). Western blotting was conducted using 2 or 10 μg of nuclear protein from RSK2$^{+/+}$ and RSK2$^{-/-}$ MEFs as indicated. The levels of phosphorylated histone H3 (Ser^{10}) and total histone H3 protein level were visualized by Western blot using specific antibodies as described in Materials and Methods. Equal protein loading was confirmed using the β-actin antibody on the same membrane.

30 μmol/L kaempferol and was almost totally blocked at 60 μmol/L kaempferol (Fig. 6*A*). However, phosphorylation of ERK induced by EGF was not changed (Fig. 6*A*), indicating that kaempferol does not affect the activity of ERK or ERK upstream kinases, including EGF receptor (EGFR), Ras/Raf, or MAPK/ERK kinase (MEK). ERK is an upstream MAPK of RSK2, which further suggests that kaempferol specifically inhibits RSK2 activity. To examine whether siRNA-RSK2 suppresses EGF-induced histone H3 phosphorylation (Ser^{10}), we introduced si-RSK2 into NIH3T3 cells and analyzed the effect of knocking down RSK2 expression. The results indicated that si-RSK2 transfection into cells suppressed EGF-induced histone H3 phosphorylation (Ser^{10}) as well as suppressing total histone H3 protein levels (Fig. 6*B*) compared with si-mock cells. However, total and phosphorylated ERK proteins were not changed in either cell line, indicating that inhibition of EGF-induced histone H3 phosphorylation in si-RSK2–transfected cells was a specific effect of RSK2 knockdown (Fig. 6*B*). To test whether RSK2 deficiency affects total histone H3 level, we assessed total protein level by Western blot in $RSK2^{+/+}$ and $RSK2^{-/-}$ MEFs. The results indicated that histone H3 protein level was lower in $RSK2^{-/-}$ MEFs compared with $RSK2^{+/+}$ MEFs (Fig. 6*C*). To analyze whether RSK2 deficiency can block EGF-induced histone H3 phosphorylation (Ser^{10}), we used 2 or 10 μg of protein from a nuclear fraction from $RSK2^{+/+}$ MEFs or $RSK2^{-/-}$ MEFs, respectively, for the Western blot analysis. The results indicated that phosphorylation of histone H3 (Ser^{10}) was very weak in $RSK2^{-/-}$ MEFs, although five times more protein was used compared with $RSK2^{+/+}$ MEFs (Fig. 6*D*). Taken together, these results provide strong evidence showing that RSK2 is a key regulator of EGF- or TPA-induced cell transformation, which might be regulated through RSK2-mediated histone H3 phosphorylation at Ser^{10}.

Discussion

Various environmental stimuli activate MAPK cascades, which regulate many cellular responses that result in the transcriptional activation of immediate-early response genes (IEG; ref. 33). The rapid induction of IEG by external stimuli is associated with the delivery of intracellular signals to transcription factors and cofactors at regulatory elements as well as nucleosomes present both at the promoter and within the transcribed region of genes (34). In particular, the Ras/ERK pathway has a critical role in regulating cell proliferation, survival, growth and motility (26, 27), and tumorigenesis (28).

The MAPKs comprise a family of proteins that mediate a series of distinct signaling cascades, which are targeted by a multitude of extracellular stimuli. Activated MAPKs translocate to the nucleus, where they phosphorylate their target molecules, including various transcription factors and histone H3 (35). Constitutive activation of MAPK-related oncogenes, such as *H-ras*, increases the level of phosphorylated H3 in mouse fibroblasts (36, 37). Several reports have confirmed that the MAPK cascades are key players in the nucleosomal response ending in the phosphorylation of H3 (Ser^{10}) and the activation of IEGs (37, 38). EGF and TPA were first reported to induce H3 phosphorylation at Ser^{10} (38, 39) and Ser^{28} (40), respectively, through the ERK pathway. Recently, we also found that the p53 tumor suppressor protein is required for RSK2-mediated histone H3 phosphorylation at Ser^{10} induced by EGF or UVB stimulation (13). Moreover, we showed that knockdown of histone H3 with siRNA inhibited EGF-induced cell transformation in JB6 Cl41 cells (32). Notably, we found that overexpression of mutant histone H3 (histone H3 S10A) in JB6 Cl41 cells inhibited EGF-induced cell transformation compared with cells overexpressing wild-type histone H3 (32).

Herein, our data indicated that RSK2 inhibition by gene knockout suppressed cell proliferation (Fig. 2*B*) and overexpression of RSK2 induced cell proliferation as well as cell transformation (Fig. 3*B* and *C*) through a Ras-dependent pathway (Fig. 4*C*). In contrast to overexpression, knockdown of RSK2 with siRNA inhibited Ras-induced foci formation in NIH3T3 cells (Fig. 4*C*). Moreover, kaempferol, a chemical inhibitor of RSK2 (Fig. 5*A*), suppressed EGF-induced transformation (Fig. 5*D*) as well as proliferation in JB6 Cl41 cells (Fig. 5*C*). Very importantly, kaempferol also suppressed EGF-induced histone H3 phosphorylation (Ser^{10}; Fig. 6*A*). In addition, EGF-induced phosphorylation of histone H3 was totally blocked in RSK2-null MEFs (Fig. 6*C*). Taken together, these results indicate that RSK2 is a critical regulator of cell transformation induced by tumor promoters, such as EGF or TPA, and the effect is mediated through the phosphorylation of histone H3 at Ser^{10} by RSK2.

Although the mechanism of RSK activation has been studied in many research models, more progress is needed to understand the biological roles of RSK2. Although several downstream substrates of RSK2, including c-Fos, Elk-1, histones, CREB, ATF4, and p53, have been identified (7–13), very little is known about the physiologic function of RSK2 and especially its role in cell transformation. Previously, we found that RSK2 overexpression in 293 cells induced S-phase accumulation, indicating that RSK2 is also involved in the G_1-S transition (13). Moreover, dominant-negative CREB, which is a downstream target of RSK2, induced G_1 accumulation and then stimulated apoptosis by attenuating DNA synthesis in response to several activation signals, such as TPA, ionomycin, or concanavalin A (41). In addition, the well-known downstream targets of RSK2 are c-Fos, CREB, and histone H3. These proteins are involved in cell proliferation as well as cell transformation (20, 32, 42). Our results showed that knockdown of RSK2 by siRNA-RSK2 almost totally suppressed focus formation in NIH3T3 cells and cell proliferation was suppressed but to a lesser degree (Fig. 4*C* and *D*). Furthermore, JB6 Cl41 cell transformation was inhibited more markedly by the RSK2 inhibitor kaempferol than was cell proliferation in the same cells (Fig. 5*C* and *D*). Kaempferol was shown to specifically inhibit RSK2 but not RSK1 or RSK3. Previous docking studies using computer modeling indicated that kaempferol can potentially form hydrogen bonds with Thr^{210} in the RSK2 NH_2-terminal ATP-binding pocket (43). In addition, RSK2, which is phosphorylated and activated by ERK, also phosphorylates histone H3 Ser^{10} (7, 8, 44, 45). We found that kaempferol did not inhibit ERK phosphorylation (Fig. 6*A*), indicating that ERKs, MEKs, Ras/Raf, and EGFR are not targets. Overall, these results indicated that inhibition of cell transformation mediated by suppressing RSK2 might be due to a suppression of cell proliferation as well as a reduction of signaling to downstream target transcription factors. RSK2 is thus a key regulator of cell transformation induced by tumor promoters such as EGF or TPA.

Acknowledgments

Received 12/22/2006; revised 4/27/2007; accepted 6/22/2007.

Grant support: Hormel Foundation and NIH grants CA120388, CA77646, CA81064, and CA111356.

The costs of publication of this article were defrayed in part by the payment of page charges. This article must therefore be hereby marked *advertisement* in accordance with 18 U.S.C. Section 1734 solely to indicate this fact.

We thank Dr. M.E. Greenberg (Division of Neuroscience, Children's Hospital, Harvard Medical School, Boston, MA) and Dr. J.A. Smith (Department of Pathology, Center for Cell Signaling, University of Virginia, Charlottesville, VA) for the RSK2 plasmid and Dr. J.C. Bruning for the $RSK2^{+/+}$ and $RSK2^{-/-}$ embryonic fibroblasts.

References

1. Sebolt-Leopold JS. Development of anticancer drugs targeting the MAP kinase pathway. Oncogene 2000;19: 6594–9.
2. Roux PP, Blenis J. ERK and p38 MAPK-activated protein kinases: a family of protein kinases with diverse biological functions. Microbiol Mol Biol Rev 2004;68: 320–44.
3. Jones SW, Erikson E, Blenis J, Maller JL, Erikson RL. A *Xenopus* ribosomal protein S6 kinase has two apparent kinase domains that are each similar to distinct protein kinases. Proc Natl Acad Sci U S A 1988;85:3377–81.
4. Frodin M, Jensen CJ, Merienne K, Gammeltoft S. A phosphoserine-regulated docking site in the protein kinase RSK2 that recruits and activates PDK1. EMBO J 2000;19:2924–34.
5. Frodin M, Gammeltoft S. Role and regulation of 90 kDa ribosomal S6 kinase (RSK) in signal transduction. Mol Cell Endocrinol 1999;151:65–77.
6. Nebreda AR, Gavin AC. Perspectives: signal transduction. Cell survival demands some Rsk. Science 1999;286:1309–10.
7. Xing J, Ginty DD, Greenberg ME. Coupling of the RAS-MAPK pathway to gene activation by RSK2, a growth factor-regulated CREB kinase. Science 1996;273:959–63.
8. Sassone-Corsi P, Mizzen CA, Cheung P, et al. Requirement of Rsk-2 for epidermal growth factor-activated phosphorylation of histone H3. Science 1999; 285:886–91.
9. Blenis J. Signal transduction via the MAP kinases: proceed at your own RSK. Proc Natl Acad Sci U S A 1993;90:5889–92.
10. Davis RJ. Transcriptional regulation by MAP kinases. Mol Reprod Dev 1995;42:459–67.
11. Ward GE, Kirschner MW. Identification of cell cycle-regulated phosphorylation sites on nuclear lamin C. Cell 1990;61:561–77.
12. Yang X, Matsuda K, Bialek P, et al. ATF4 is a substrate of RSK2 and an essential regulator of osteoblast biology; implication for Coffin-Lowry Syndrome. Cell 2004;117: 387–98.
13. Cho YY, He Z, Zhang Y, et al. The p53 protein is a novel substrate of ribosomal S6 kinase 2 and a critical intermediary for ribosomal S6 kinase 2 and histone H3 interaction. Cancer Res 2005;65:3596–603.
14. Hunter T, Karin M. The regulation of transcription by phosphorylation. Cell 1992;70:375–87.
15. Angel P, Imagawa M, Chiu R, et al. Phorbol ester-inducible genes contain a common *cis* element recognized by a TPA-modulated *trans*-acting factor. Cell 1987;49:729–39.
16. Sachsenmaier C, Radler-Pohl A, Zinck R, Nordheim A, Herrlich P, Rahmsdorf HJ. Involvement of growth factor receptors in the mammalian UVC response. Cell 1994;78:963–72.
17. Ben-Ari ET, Bernstein LR, Colburn NH. Differential c-jun expression in response to tumor promoters in JB6 cells sensitive or resistant to neoplastic transformation. Mol Carcinog 1992;5:62–74.
18. Dong Z, Birrer MJ, Watts RG, Matrisian LM, Colburn NH. Blocking of tumor promoter-induced AP-1 activity inhibits induced transformation in JB6 mouse epidermal cells. Proc Natl Acad Sci U S A 1994;91:609–13.
19. Bonni A, Brunet A, West AE, Datta SR, Takasu MA, Greenberg ME. Cell survival promoted by the Ras-MAPK signaling pathway by transcription-dependent and -independent mechanisms. Science 1999;286:1358–62.
20. David JP, Mehic D, Bakiri L, et al. Essential role of RSK2 in c-Fos-dependent osteosarcoma development. J Clin Invest 2005;115:664–72.
21. Smith JA, Poteet-Smith CE, Xu Y, Errington TM, Hecht SM, Lannigan DA. Identification of the first specific inhibitor of p90 ribosomal S6 kinase (RSK) reveals an unexpected role for RSK in cancer cell proliferation. Cancer Res 2005;65:1027–34.
22. Clark DE, Errington TM, Smith JA, Frierson HF, Jr., Weber MJ, Lannigan DA. The serine/threonine protein kinase, p90 ribosomal S6 kinase, is an important regulator of prostate cancer cell proliferation. Cancer Res 2005;65:3108–16.
23. Colburn NH, Wendel EJ, Abruzzo G. Dissociation of mitogenesis and late-stage promotion of tumor cell phenotype by phorbol esters: mitogen-resistant variants are sensitive to promotion. Proc Natl Acad Sci U S A 1981;78:6912–6.
24. Clark GJ, Cox AD, Graham SM, Der CJ. Biological assays for Ras transformation. Methods Enzymol 1995; 255:395–412.
25. Sebolt-Leopold JS, Herrera R. Targeting the mitogen-activated protein kinase cascade to treat cancer. Nat Rev Cancer 2004;4:937–47.
26. Pearson G, Robinson F, Beers Gibson T, et al. Mitogen-activated protein (MAP) kinase pathways: regulation and physiological functions. Endocr Rev 2001;22:153–83.
27. Schaeffer HJ, Weber MJ. Mitogen-activated protein kinases: specific messages from ubiquitous messengers. Mol Cell Biol 1999;19:2435–44.
28. Cho YY, Bode AM, Mizuno H, Choi BY, Choi HS, Dong Z. A novel role for mixed-lineage kinase-like mitogen-activated protein triple kinase α in neoplastic cell transformation and tumor development. Cancer Res 2004;64:3855–64.
29. Miean KH, Mohamed S. Flavonoid (myricetin, quercetin, kaempferol, luteolin, and apigenin) content of edible tropical plants. J Agric Food Chem 2001;49: 3106–12.
30. Cohen MS, Zhang C, Shokat KM, Taunton J. Structural bioinformatics-based design of selective, irreversible kinase inhibitors. Science 2005;308:1318–21.
31. Cho YY, Yao K, Bode AM, et al. RSK2 mediates muscle cell differentiation through regulation of NFAT3. J Biol Chem 2007;282:8380–92.
32. Choi HS, Choi BY, Cho YY, et al. Phosphorylation of histone H3 at serine 10 is indispensable for neoplastic cell transformation. Cancer Res 2005;65:5818–27.
33. Treisman R. Regulation of transcription by MAP kinase cascades. Curr Opin Cell Biol 1996;8:205–15.
34. Hazzalin CA, Mahadevan LC. MAPK-regulated transcription: a continuously variable gene switch? Nat Rev Mol Cell Biol 2002;3:30–40.
35. Bode AM, Dong Z. Inducible covalent posttranslational modification of histone H3. Sci STKE 2005; 2005:re4.
36. Chadee DN, Hendzel MJ, Tylipski CP, et al. Increased Ser-10 phosphorylation of histone H3 in mitogen-stimulated and oncogene-transformed mouse fibroblasts. J Biol Chem 1999;274:24914–20.
37. Strelkov IS, Davie JR. Ser-10 phosphorylation of histone H3 and immediate early gene expression in oncogene-transformed mouse fibroblasts. Cancer Res 2002;62:75–8.
38. Cheung P, Tanner KG, Cheung WL, Sassone-Corsi P, Denu JM, Allis CD. Synergistic coupling of histone H3 phosphorylation and acetylation in response to epidermal growth factor stimulation. Mol Cell 2000;5:905–15.
39. Ota T, Suto S, Katayama H, et al. Increased mitotic phosphorylation of histone H3 attributable to AIM-1/Aurora-B overexpression contributes to chromosome number instability. Cancer Res 2002;62:5168–77.
40. Soloaga A, Thomson S, Wiggin GR, et al. MSK2 and MSK1 mediate the mitogen- and stress-induced phosphorylation of histone H3 and HMG-14. EMBO J 2003;22: 2788–97.
41. Barton K, Muthusamy N, Chanyangam M, Fischer C, Clendenin C, Leiden JM. Defective thymocyte proliferation and IL-2 production in transgenic mice expressing a dominant-negative form of CREB. Nature 1996; 379:81–5.
42. Conkright MD, Montminy M. CREB: the unindicted cancer co-conspirator. Trends Cell Biol 2005;15:457–9.
43. Nguyen TL, Gussio R, Smith JA, et al. Homology model of RSK2 N-terminal kinase domain, structure-based identification of novel RSK2 inhibitors, and preliminary common pharmacophore. Bioorg Med Chem 2006;14:6097–105.
44. Smith JA, Poteet-Smith CE, Malarkey K, Sturgill TW. Identification of an extracellular signal-regulated kinase (ERK) docking site in ribosomal S6 kinase, a sequence critical for activation by ERK *in vivo*. J Biol Chem 1999; 274:2893–8.
45. Roux PP, Richards SA, Blenis J. Phosphorylation of p90 ribosomal S6 kinase (RSK) regulates extracellular signal-regulated kinase docking and RSK activity. Mol Cell Biol 2003;23:4796–804.

Ribosomal S6 Kinase 2 Is a Key Regulator in Tumor Promoter–Induced Cell Transformation

Yong-Yeon Cho, Ke Yao, Hong-Gyum Kim, et al.

Cancer Res 2007;67:8104-8112.